

Document downloaded from:

<http://hdl.handle.net/10251/56993>

This paper must be cited as:

Vidal Pantaleoni, A.; Moreno Cambroreno, MDR. (2011). Change detection of isolated housing using a new hybrid approach based on object classification with optical and TerraSAR-X data. International Journal of Remote Sensing. 32(24):9621-9635.  
doi:10.1080/01431161.2011.571297.



The final publication is available at

<http://dx.doi.org/10.1080/01431161.2011.571297>

Copyright Taylor & Francis (Routledge): STM, Behavioural Science and Public Health Titles

Additional Information

# Change detection of isolated housing using a new hybrid approach based on object classification with optical and TerraSAR-X data

A. Vidal\*\*and M. R. Moreno  
iTEAM, Universidad Politécnica de Valencia  
C. de Vera s/n, E-46022 Valencia, Spain

Received March 2010

## Abstract

Optical and microwave high spatial resolution images are now available for a wide range of applications. In this work, they have been applied for the semi-automatic change detection of isolated housing in agricultural areas. This paper presents a new hybrid methodology based on segmentation of high resolution images and image differencing. This new approach mixes the main techniques used in change detection methods and it also adds a final segmentation process in order to classify the change detection product. First, isolated building classification is carried out using only optical data. Then, Synthetic Aperture Radar (SAR) information is added to the classification process, obtaining excellent results with lower complexity cost. Since the first classification step is improved, the total change detection scheme is also enhanced when the radar data is used for classification. Finally, a comparison between the different methods is presented and some conclusions are extracted from the study.

## 1 Introduction

The detection of man-made structures using remote sensing is a very interesting application for governments and town councils. This task, that is

---

\*\*Corresponding author. Email: [avidal@dcom.upv.es](mailto:avidal@dcom.upv.es)

useful for periodic inventory of land use and also for monitoring illegal construction, may be carried out using aerial or high spatial resolution satellite data. Traditionally, this work has been carried out using aerial images in the optical domain and visual interpretation. This method is very rigorous, but it is also very time-consuming and it needs a human operator. In this study, a new semi-automatic hybrid process using data in the optical and microwave domains is proposed. The final goal is to help a human operator in order to reduce the overall processing time in the task of monitoring illegal construction in agricultural areas, which usually comes in the form of isolated housing.

Remote sensing data may be acquired by active or passive systems. Active sensors like radar present some advantages over passive systems. Probably, the most important one is that radar operation does not depend on solar illumination and weather conditions. Radar images also present an interesting characterization of man-made structures, due to the electrical properties of construction elements like concrete, which are very different from other natural surfaces. The main advantage of optical imagery coming from passive systems is that it is easier to be understood by human operators, and geophysical models in the optical domain are more robust. However, the challenge consists in the combination of both sources of information in order to collect their main advantages and to improve the application under consideration.

TerraSAR-X is a German Synthetic Aperture Radar (SAR) satellite mission with scientific and commercial applications, which was launched in 2007. It is a public-private partnership between the German Aerospace Center (DLR) and Astrium. The main instrument is an active phased array X-Band system, with a center frequency of 9.65 GHz. The radar can use different polarization and imaging modes with different resolution and coverage, shown in table 1: SpotLight (SL), High Resolution SpotLight (HS), StripMap and ScanSAR Fritz and Eineder (2009). In this work we have not explored the polarimetric possibilities that TerraSAR-X offers because we were interested in very high spatial resolution products.

[Insert table 1 around here]

A large number of applications using the unique capabilities of TerraSAR-X are proposed in Scheuchl *et al.* (2009). Some works have already been reported in the literature for simple land cover classification trying to detect urban areas from water, forestry or agricultural fields Eschm *et al.* (2006). However, the problem which is proposed in this paper is different, since single building contours are more difficult to be detected than coarse highly populated areas like villages or towns. General land cover classification with TerraSAR-X is also studied in Burini *et al.* (2008) including other sources of

data like SPOT images and other ancillary data.

There are several methods to carry out classification and change detection. However, single building detection usually requires very high spatial resolution images and an object-based supervised classifier Aplin and Smith (2008). This approach has been applied successfully in urban detection not only with aerial optical imagery Estornell *et al.* (2004); Hermosilla *et al.* (2008), but also with high spatial resolution satellite imagery in the optical domain, such as Quickbird and IKONOS Bauer and Steinnocher (2001); Herold *et al.* (2002) and with more moderate spatial resolution like ASTER (Advanced Spaceborne Thermal Emission and Reflection Radiometer) imagery Chen *et al.* (2007). Recent studies have described different approaches to classify individual housing from very high resolution imagery, by means of semi-automatic methods based on variance filters combined with additional data, like shadow information or vegetation information. In this manner, single buildings that correspond to certain shapes and sizes are identified and reconstructed Lhomme *et al.* (2009). However, all these approaches do not employ data from microwave sensors like TerraSAR-X.

There are several strategies in the change detection algorithms. Change detection methods can be basically divided in two classes: map-to-map methods and image-to-image methods Lu *et al.* (2004); Han *et al.* (2008); Dalla *et al.* (2008); Im *et al.* (2008). A map-to-map method includes a classification step. An image-to-image comparison method usually includes: differencing, ratio-ing, regression, Principal Component Analysis (PCA) and Change Vector Analysis (CVA). Change detection based on CVA is usually applied to low and medium resolution imagery where geometric and textural information do not provide enough information Dalla *et al.* (2008).

The combination of SAR and optical information has already been applied in some fields. SAR images involves an important source of textural information that can be applied to improve the classification of land cover Shimabukuro *et al.* (2007), crop types Lobo and Chic (1996); Blaes *et al.* (2005) or urban environment. Residential areas present isolated backscattering elements, double bounce reflection and shadows, whereas town centers are characterized by mixed backscattering environments. In this manner, SAR data from ENVISAT and RADARSAT have already been used to classify vegetation, water, city centers, high-density urban areas, residential and medium-density areas and suburban zones Dell'Acqua and Gamba (2006). Some studies have investigated urban change detection using 3D models by means of SAR simulators, or in earthquake damage detection applying pixel to pixel difference Stramondo *et al.* (2006). However, previous research did not use very high resolution SAR images for the problem under consideration.

In this work, a novel change detection application based on segmentation

has been carried out using very high resolution SAR and optical data for the detection of new isolated housing in rural areas. This paper focuses on a new hybrid methodology for the semi-automatic change detection of buildings, based on the object-based classification applied at different steps of the processing chain. Besides, the study introduces the innovative combination of very high spatial resolution in the microwave and the optical domains.

## 2 Study area and data

The study site is located in Benicarló (Spain), a coastal area in the North of the Comunidad Valenciana. In this region, town councils are very interested in monitoring illegal construction in agricultural areas because it can involve important problems. On the one hand, rural areas have not infrastructures, roads or sewer systems, so illegal construction could bring an increased risk of rubbish dump, fire hazard or water contamination. On the other hand, illegal construction constitutes a crime that should be prosecuted. Remote sensing, in the form of aerial high resolution optical images, is already being used by human operators in gubernamental agencies. However, a semi-automatic tool that could help in the visual inspection would be very interesting for this task.

For this work, the following material has been used:

- Two very high spatial resolution ortho-rectified aerial images in the optical domain. The images are composed of the three Red Green and Blue (RGB) bands: Blue ( $0.4 \mu\text{m}$  to  $0.5 \mu\text{m}$ ), Green ( $0.5 \mu\text{m}$  to  $0.6 \mu\text{m}$ ), Red ( $0.6 \mu\text{m}$  to  $0.7 \mu\text{m}$ ). They were acquired in July of 2003 and August of 2007 and they present a spatial resolution of  $0.5 \text{ m}$ .
- One high resolution SAR image captured with the TerraSAR-X satellite on 30th March 2009. The image used in our study is a SpotLight image with pixel spacing of  $0.75 \text{ m}$  and Horizontal-Horizontal (HH) single mode polarization. The chosen product provided by German DLR has used the Enhanced Ellipsoid Corrected (EEC) and Spatially Enhanced (SE) options.
- Cadastral information provided by local governmental agencies, which gives parcel polygonal information.

### 3 Methodology

Geometric corrections are very important in all change detection and fusion algorithms. In this case, the 2007 optical scene is taken as a reference and the rest of images have been adjusted to fit this reference (see figure 1). The SAR image and the 2003 optical image were co-registered by locating ground control points (GCPs) with respect to the reference image. Ground control points (GCP) were selected manually after a visual identification of common objects in both images. Logically, the visual identification of GCPs in the SAR image was more difficult and time consuming because it presented information of different nature with different pixel size. In this study, twenty-two ground control points were identified at each scene. Then, the spatial transformation was defined using a first order polynomial and the nearest neighbor method for resampling. Since the optical image and the radar image presented different spatial resolution, they were merged by the interpolation of the radar image using the nearest neighbor technique again.

[Insert figure 1 around here]

Radiometric corrections were only carried out in the 2003 RGB image. There are several options for rigorous radiometric correction Yuan and Elvidge (1996). However, in this study the radiometric adjustment has only taken into account the pixels that are classified as buildings in the 2007 RGB image. This technique tries to adjust the statistics of the spectral levels of the isolated building roofs, that present different values at different dates due to the changing illumination and atmospheric conditions.

In this paper, a novel mixed approach between object processing, classification and mathematical operations is proposed (see figure 1). First, the most recent image (2007) is classified because it is more common to build buildings than to demolish them. Then, image subtraction is performed only on the areas classified as buildings (see figure 1). Classification is the most time-consuming step in the processing chain, so if only one scene is classified, the overall processing time decreases considerably. The first task is then to detect all the buildings in the most recent image taken in 2007. This is achieved by object classification using the Feature Extraction module from the ENVI software (ITT Visual Information Solutions). Basically, the two main steps are segmentation and classification. Image segmentation is based on the clustering of adjacent pixels according to their spectral and geometric characteristics. The segmentation algorithm uses an edge-based technique. For that reason, only one threshold is needed (Scale Level). This percentage is adjustable; it depends on the image, the number of bands, the area size, the illumination of the scene and other parameters. In this way, the image is divided into separated regions, named objects.

An object contains not only different spectral data but also spatial and textural information. Then, object classification is carried out according to all these attributes. The final objective in this work has been to detect buildings from other land covers. Therefore, a binary classification or detection has been carried out. An object may be labelled as “building” or “not building” according to some rules that are defined by a combination of spectral and spatial attributes. However, as an intermediate step, different classes of buildings have been defined because they can present very different characteristics in shape, size and spectral information. First, some groups of buildings are identified and special rules are created for them. Then, all groups are joined into a unique class. Specifications of all the attributes that can be used by the software are included in table 2.

[Insert table 2 around here]

Anyway, not all the attributes are needed to define the best classification rule in figure 1. The results do not improve by using more attributes, the performance of a rule depends on the best combination of the necessary attributes. To define the classification with the Red-Green and Blue bands (RGB rule), the following attributes have been employed (spectral information of RGB bands, Area, Elongation, Compact, Rectangular-fit, Solidity and Hole density). Spectral attributes are divided in four blocks, for each band we can work with the Standard deviation, Minimum value (Min), Maximum value or Average value. Therefore, if three bands are considered, there is a total of twelve spectral attributes to be combined. However, the study has shown that the Average value for each of the bands was sufficient. This attribute has a range with a minimum value equal to zero and a maximum value equal to 255. The Area attribute estimates the size of each individual object, subtracting the area of the holes. So, tiny or huge objects can be easily eliminated from the classification. Rectangular-fit attribute is a measure of the similarity of the object with a rectangle. This attribute is obtained by means of an equation that compares the area with the length of the major and the minor axis of the bounding box enclosing the polygon. Hole density attribute evaluates the number and the size of the holes inside an object. Compact attribute compares the area of the objects with the length of the outer contour. Solidity attribute compares the area of the objects with the area of the convex hull. Finally, Elongation attribute compares the major axis of the polygon with the minor axis. This attribute is quite useful to eliminate the roads from the building classification.

Next step considers the usage of the SAR image into the processing chain (see figure 1) in order to explore the possible advantages of radar images in classification of urban areas. One of the major problems that we found was the speckle noise of the image. It covers all the structures and causes grey

value variations in the image as it can be seen in figure 2(b). In this case, the SAR image is not very clear, only the roads and some buildings are visible with very low backscattering values. However, SAR data may be of interest to help the classification process that may be very complicated when the building roofs somehow coincide in the visible range with the surrounding soil. Therefore, the SAR image is processed in order to reduce the speckle noise. This pre-processing can improve the final results and it can help to identify image segments that represent real structures. There are several adaptive spatial filters that have been applied for speckle reduction in the literature: Lee, Kuan, Frost, Enhanced Lee, Frost, Gamma filter and others. Some studies have also employed the Mean Filter Eschm *et al.* (2006) or the Lee-Sigma filter Xiao-Xia *et al.* (2006). Most of the speckle reduction filters must assume a trade-off between noise reduction and detail preservation, since the low-pass filters tend to obtain a smooth version of the image. In the original SAR image, built areas present low backscattering values. Therefore, our objective is to smooth the backscattering values as much as possible, meanwhile dark area boundaries, where buildings are located, are preserved. For that purpose, a median filter has been chosen. Next, a logarithmic transformation is applied in order to equalize the data. The post-processed SAR image is shown in figure 2(c).

[Insert figure 2 around here]

This processed image is introduced in the building classification of the 2007 image carried out before using only the RGB bands (see figure 1). The segmentation step is preserved, but the attribute information now contains the backscattering value as an extra band. The building classification using the SAR band is excellent, since it gets better accuracy results with lower complexity and computation costs. The classification rule used in the case of optical images is the addition of six subrules as shown in the following equation.

$$\text{Rule}_{\text{RGB}} = \text{Subrule}_{1a} + \text{Subrule}_{2a} + \text{Subrule}_{3a} + \text{Subrule}_{4a} + \text{Subrule}_{5a} + \text{Subrule}_{6a} \quad (1)$$

Each subrule combines the previously presented attributes limited by a lower threshold, an upper threshold or both of them. Each contribution is joined by means of logical conjunction. The first subrule that involves six attributes and 10 variables to be adjusted is shown as an example in the following equation:

$$\begin{aligned} \text{Subrule}_{1a} = & (\text{Area} \in [y_1, y_2]) \ \& (\text{Average}_{\text{band}1} \in [y_3, y_4]) \ \& \\ & (\text{Average}_{\text{band}2} \in [y_5, y_6]) \ \& (\text{Average}_{\text{band}3} \in [y_7, y_8]) \ \& \\ & (\text{Elongation} < y_9) \ \& (\text{Compact} > y_{10}) \end{aligned} \quad (2)$$

The six subrules presented in equation (1) need the adjustment of a total number of variables  $y_i$  equal to 56.

By adding the extra SAR band to the process, the complexity of the classification rule decreases considerably. The attributes employed in this case are Average of each band, Minimum value of the SAR band, Area, Elongation and Compact. They are combined in a final equation structured in two subrules that involve 7 attributes and 14 variables to be adjusted  $x_i$ . The RGB-SAR final rule is shown in the following equations.

$$\text{Rule}_{\text{RGB-SAR}} = \text{Subrule}_{1b} + \text{Subrule}_{2b} \quad (3)$$

$$\begin{aligned} \text{Subrule}_{1b} = & (\text{Area} \in [x_1, x_2]) \ \& (\text{Average}_{\text{band}3} \in [x_3, x_4]) \ \& \\ & (\text{Average}_{\text{band}4} < x_5) \ \& (\text{Min}_{\text{band}4} < x_6) \ \& \\ & (\text{Elongation} < x_7) \ \& (\text{Compact} > x_8) \end{aligned} \quad (4)$$

$$\begin{aligned} \text{Subrule}_{2b} = & (\text{Area} \in [x_9, x_{10}]) \ \& (\text{Average}_{\text{band}1} > x_{11}) \ \& \\ & (\text{Average}_{\text{band}4} < x_{12}) \ \& (\text{Elongation} < x_{13}) \ \& \\ & (\text{Compact} > x_{14}) \end{aligned} \quad (5)$$

Obviously, the final classification rule becomes simpler and more flexible with the use of radar data.

Once the optical images of 2003 and 2007 are co-registered and normalized, a new product is obtained by means of the difference between the 2007 RGB image and the 2003 RGB image, both masked by the building vector obtained from the classification step, that can be obtained just with RGB data or with RGB-SAR data. Next, this change image is post-processed again by an object-based classification in order to detect the final change in binary format. The attributes that are taken into consideration are related to the shape and size of the objects, joined with their mean difference value. This is a very simple procedure that helps to decrease the false alarm rates (see figure 1).

## 4 Results

The results obtained from the proposed methodology are presented. The selected algorithm has been designed using as a model the isolated buildings of a Training zone. Then, this algorithm without any modification has been applied to three additional zones, that have not been used for training. By this procedure, results are more representative, because they have been obtained without previous knowledge of the zone under consideration. Obviously, the classification rules can not be extrapolated to any type of terrain and scene, but human operator work can be reduced by defining some typical scenarios and designing an appropriate algorithm for each of them. Figure 3 shows

the four zones of study which represent 1.2 km<sup>2</sup>, where the Training zone has been stressed in red color. This area is especially interesting because there are a lot of changes between 2003 and 2007, and it presents a variety of buildings with different spectral and spatial characteristics. Once the classification rules are defined, we apply them to the total scene, made up by the training zone plus the other three zones with similar dimensions to the training one. All them belong to the same original optical image acquired in 2007 and they present a similar environment: a rural area with individual houses and without industrial facilities or large residential buildings.

[Insert figure 3 around here]

There are two separate processes that must be evaluated. The first one is the building classification and the second one is the final change detection. For both of them, the 2003 and 2007 RGB images are visually inspected and the buildings and the urban change detection are totally mapped. This gives the true values for comparison and algorithm assessment. However, this process is slightly subjective because in some cases, there is not a clear building or a change. Perhaps a building has suffered a minor change like the roof material or a new small construction. In those cases, the involved object/parcel is labelled as “no change” in the true change detection data.

For the accuracy measurements, two rates are defined: detection rate and false alarm rate. Detection rate measures the percentage of true changes detected. On the other hand, false alarm rate considers over-detection or false changes. Logically, detection rates should be high and false alarm rates should be low. Additionally, the rates may be assessed counting number of pixels, objects or parcels. One of the most useful index is the one made on parcels that come from the cadastral information. It was employed to evaluate building classification, in that way, parcels were labelled as “built” or “not built”. Whereas, to assess urban change detection, the object criterion was chosen.

Figure 4 presents an example of a detail of the building classification results using RGB bands and RGB-SAR bands. This figure shows the contour of the objects that have been classified as buildings. Statistics in building classification using the per parcel approach are presented in table 3. Results obtained with the RGB image and the RGB-SAR data are shown by zones. This table presents an improvement of the detection accuracy when SAR data is employed. This improvement is even more relevant when the lower complexity of the new procedure using SAR data is taken into account. If the different zone results are evaluated, we see that all zones present homogeneous values and, in some cases (RGB-SAR in zone 2), the accuracy measurement is surprisingly better in a non-trained zone than in the training area.

The use of the SAR band in the process, improves the accuracies in building classification between 2% and 11%, depending on the area of study. The detection of all the buildings in a scene is a very difficult goal and it would increase the false alarm rate too. However, accuracies around 90% can be considered a very successful result. This improvement is due to the information provided by the post-processed SAR band (see figure 2), where buildings are clearly different from surrounding fields. SAR data is useful to detect houses that have been missed using just the RGB bands. Buildings may present very different appearance, shape and color. In some cases, building spectral content may be very similar to the spectral information of the land around them. The great advantage introduced by the SAR band is the possibility of distinguish between buildings and non man-made objects like trees, crop lands and others. Besides, the radar band improves its performance with the size of the house. Therefore, it is especially useful for identifying middle-high size buildings, which is just the target size of the typical illegal construction in the region under study. Finally, the improvement in classification accuracies leads to a corresponding improvement in the final change detection results.

[Insert figure 4 around here]

[Insert table 3 around here]

Once the building classification has been evaluated, the urban change detection given by RGB and RGB-SAR data are studied. In figure 5, results on change detection using RGB-SAR data are visually presented for the same area shown in figure 4. In this small area, the changes detected with and without SAR band are the same. This figure clearly shows two new houses and another house where the roof color has clearly changed from 2003 and 2007.

[Insert figure 5 around here]

Table 4 presents summary information on detection and false alarm rates for the RGB and the RGB-SAR solution counting objects. Results are shown for the Training zone and for all the studied areas (including the Training zone and the other three additional zones). The addition of the SAR band clearly improves the change detection results in both detection rate and false alarm rate values. Moreover, this trend is confirmed in the blind change detected zones, giving excellent results with low complexity. In the Training area, the detection rate using SAR band improves approximately 14%, whereas the false alarm rate decreases 4%. The test on the total area provides similar results, an increase of the detection rate of 17% and a decrease of 6% in the false alarm rate. This improvement comes from the fact that initial classification results are better using the SAR band. Logically, when more buildings are detected in the recent image, then more changes may be

identified later.

[Insert table 4 around here]

Figure 6 visually presents another portion of the image, where the results obtained in the final change detection, adding the SAR band, are slightly different from the results obtained using only the RGB bands.

[Insert figure 6 around here]

## 5 Conclusions

This study has proposed a new hybrid object-oriented urban change detection technique using very high resolution SAR and optical images for monitoring illegal construction. A new change detection strategy has been designed, using object-oriented classification at different steps of the algorithm, and mixed with the classical subtraction of masked images. Objects obtained after segmentation do not only provide spectral information, but also shape and texture information. The method gets high accuracy values with RGB data even for the blind classification, but it gets even more promising when very high resolution TerraSAR-X images are included in the procedure.

Building classification results are excellent in the RGB-SAR method. Obviously, if the classification gets better, then the change detection results are also improved. In that case, there is an increase of the detection rate over 17% and the false alarm rate also gets 6% lower with the incorporation of the SAR band to the process. Besides, there are additional factors that make a difference between the two methods. Not only the accuracy improves, but the method also gets simpler and the computation time decreases when the SAR image is employed. The complexity of the classification rule for the RGB solution is quite high, whereas the RGB-SAR composition requires a very simple rule defined with a small number of variables. Moreover, the simplicity in defining the classification rules makes easier its extension to other possible scenarios.

As a final conclusion, very high resolution radar images like TerraSAR-X images are an excellent complement to optical high resolution images for carrying out isolated housing change detection.

## 6 Acknowledgments

The authors would like to thank the “Instituto Cartográfico de Valencia” for the provision of aerial images. They also want to thank the German Aerospace Center (DLR), that provided the TerraSAR-X data in the frame

of a Scientific Use agreement.

## References

- APLIN, P. and SMITH, G.M., 2008, Advances in object-based classification. *International Archives of the Photogrammetry, Remote Sensing and Spatial Information Sciences*, **37**, pp. 725–728.
- BAUER, T. and STEINNOCHER, K., 2001, Per-parcel land use classification in urban areas applying a rule-based technique. *GeoBit/GIS*, **6**, pp. 24–27.
- BLAES, X., VANHALLE, L. and DEFOURNY, P., 2005, Efficiency of crop identification based on optical and SAR image time series. *Remote Sensing of Environment*, **96**, pp. 352–365.
- BURINI, A., PUTIGNANO, C., DEL FRATE, F., LICCIARDI, G., PRATOLA, C., SCHIAVON, G. and SOLIMINI, D., 2008, TerraSAR-X/SPOT-5 Fused Images for Supervised Land Cover Classification. In *Proceedings of the Geoscience and Remote Sensing Symposium. IGARSS 2008*, 7–11 July 2008, Boston, US, pp. 373–376.
- CHEN, Y., SHIT, P., FUNG, T., WANG, J. and LI, X., 2007, Object-oriented classification for urban land cover mapping with ASTER imagery. *International Journal of Remote Sensing*, **28**, pp. 4645–4651.
- DALLA, M., ATLI, J., BOVOLO, F. and BRUZZONE, L., 2008, An unsupervised technique based on morphological filters for change detection in very high resolution images. *IEEE Geoscience and Remote Sensing Letters*, **5**, pp. 433–437.
- DELL'ACQUA, F. and GAMBA, P., 2006, Discriminating urban environments using multiscale texture and multiple SAR images. *International Journal of Remote Sensing*, **27**, pp. 3797–3812.
- ESCHM, T., ROTH, A. and DECH, S., 2006, Analysis of Urban Land Use Pattern Based on High Resolution Radar Imagery. In *Proceedings of the Geoscience and Remote Sensing Symposium. IGARSS 2006*, 31 July–4 August 2006, Denver, US, pp. 3615–3618.
- ESTORNELL, J., RUIZ, L.A. and DEL REY, A., 2004, Análisis metodológico para la detección de cambios urbanos en la ciudad de Valencia. *Revista de Teledetección*, **22**, pp. 55–56.
- FRITZ, T. and EINEDER, M., 2009, TerraSAR-X Ground Segment Basic Product Specification Document. Technical report, DLR, Doc.:TX-GS-DD-3302.
- HAN, S.S., LI, H.T. and GU, H.Y., 2008, The study of land use change detection based on object-oriented analysis. In *Proceedings of the International Workshop on Earth observation and Remote Sensing Applications*, pp. 1–6.
- HARALICK, R.M., SHANMUGAM, K. and DINSTEIN, I., 1973, Textural Features for Image Classification. *IEEE Transactions on Systems, Man and Cybernetics*, **3**, pp. 610–621.

- HERMOSILLA, T., RUIZ, L.A., SARRIÁ, A.F. and RECIO, J.A., 2008, Detección automática de edificios en imágenes áreas mediante técnicas de teledetección y análisis contextual. *Congreso Internacional sobre Ingeniería Geomática y Topográfica, TOPCART 2008*.
- HEROLD, M., SCEPAN, J., MLLER, A. and GNTHER, S., 2002, Object-oriented mapping and analysis of urban land use/cover using IKONOS data. In *Proceedings of the 22nd EARSeL Symposium*, Prague.
- IM, J., JENSEN, J.R. and TULLIS, J., 2008, Object-based change detection using correlation image analysis and image segmentation. *International Journal of Remote Sensing*, **29**, pp. 399–423.
- LHOMME, S., HE, D.C., WEBER, C. and MORIN, D., 2009, A new approach to building identification from very-high-spatial-resolution images. *International Journal of Remote Sensing*, **30**, pp. 1341–1354.
- LOBO, A. and CHIC, O., 1996, Classification of Mediterranean crops with multisensor data: per-pixel versus per-object statistics and image segmentation. *International Journal of Remote Sensing*, **17**, pp. 2385–2400.
- LU, D., MAUSEL, P., BRONDIZIO, E. and MORAN, E., 2004, Change detection techniques. *International Journal of Remote Sensing*, **25**, pp. 2365–2407.
- SCHEUCHL, B., KOUDOGBO, F., PETRAT, L. and PONCET, F., 2009, TerraSAR-X: Applications for Spaceborne High Resolution SAR Data. In *Proceedings of the XIV Simposio Brasileiro de Sensoriamento Remoto*, 25–30 April 2009, Natal, Brasil (INPE), pp. 7457–7464.
- SHIMABUKURO, Y., ALMEIDA-FILHO, R., M.KUPLICH, T. and DE FREITAS, R.M., 2007, Quantifying optical and SAR image relationships for tropical landscape features in the Amazonia. *International Journal of Remote Sensing*, **28**, pp. 3831–3840.
- STRAMONDO, S., BIGNAMI, C., CHINI, M., PIERDICCA, N. and TERTULLIANI, A., 2006, Satellite radar and optical remote sensing for earthquake damage detection: results from different case studies. *International Journal of Remote Sensing*, **27**, pp. 4433–4447.
- XIAO-XIA, S., JI-XIAN, Z., ZHENG-JUN, L. and ZHENG, Z., 2006, Classification from airborne SAR data enhanced by optical image using and object-oriented approach. In *Proceedings of the ISPRS Symposium on Remote Sensing: From pixels to processes*.
- YUAN, D. and ELVIDGE, C.D., 1996, Comparison of relative radiometric normalization techniques. *ISPRS Journal of Photogrammetry and Remote Sensing*, **51**, pp. 117–126.

Table 1: TerraSAR-X imaging modes.

	SpotLight Mode		StripMap Mode		ScanSAR Mode
Polarization	Single: HH or VV	Dual: HH/VV	Single: HH or VV	Dual: HH/VV, HH/HV	Single: VV or VV/VH
Scene dimension (km×km)	10×10 (SL) 10×5 (HS)	10×10 (SL) 10×5 (HS)	50×30	50×15	150×100
Azimuth resolution (m)	1.70 (SL) 1.10 (HS)	3.40 (SL) 2.20 (HS)	3.30	6.60	18.50

Table 2: Object-based attributes.

Type	Description	
Spectral	Standard deviation, Minimum, Maximum and Average of the pixels in the band	
Textural	Range, Mean, Variance and Entropy of the pixels comprising the region inside a kernel Haralick <i>et al.</i> (1973).	
	Area	Area of the polygon minus area of the holes.
	Length	Length of the boundaries of the polygon and the holes.
	Compactness	$\frac{\sqrt{4\text{Area}}}{L}$ where $L$ = length of the outer contour.
	Convexity	(Length of convex hull)/Length
	Solidity	Area/(Area of convex hull)
	Majaxislen	Length of the major axis of an oriented bounding box enclosing the polygon.
Spatial	Minaxislen	Length of the minor axis of an oriented bounding box enclosing the polygon.
	Roundness	$4 \text{ Area } /(\pi \text{ Majaxislen}^2)$
	Formfactor	$4\pi\text{Area}/\text{Perimeter}^2$
	Elongation	Indicates the ratio of the major axis of the polygon to the minor axis of the polygon.
	Rectangular Fit	Indicates how well the shape is described by a rectangle: Area/(Majaxislen $\times$ Minaxislen).
	Maindir	Angle subtended by the major axis of the polygon and the horizontal axis in degrees.
	Number of holes	Integer value that indicates the number of holes in the polygon.
	Hole density	Area/(outer contour area)
Color	Hue	Color filter angle from $0^\circ$ to $360^\circ$ .
	Saturation	Color filter depth in floating-point (0 to 1.0).
	Intensity	Measure of brightness in floating-point (0 to 1.0).
Band ratio	Normalized band ratio between two bands B1 and B2: $(B2-B1)/(B2 + B1)$ .	

Table 3: Per parcel detection accuracy (%) in building classification.

	Training Zone	Zone 2	Zone 3	Zone 4
RGB-SAR	86.79	93.51	84.50	86.26
RGB	84.90	82.44	83.09	79.12

Table 4: Per object change detection accuracy (%).

		<b>Training zone</b>	<b>All zones</b>
RGB-SAR	Detection rate	95.83	94.83
	False Alarm rate	4.16	16.66
RGB	Detection rate	81.48	77.77
	False Alarm rate	8.30	22.22

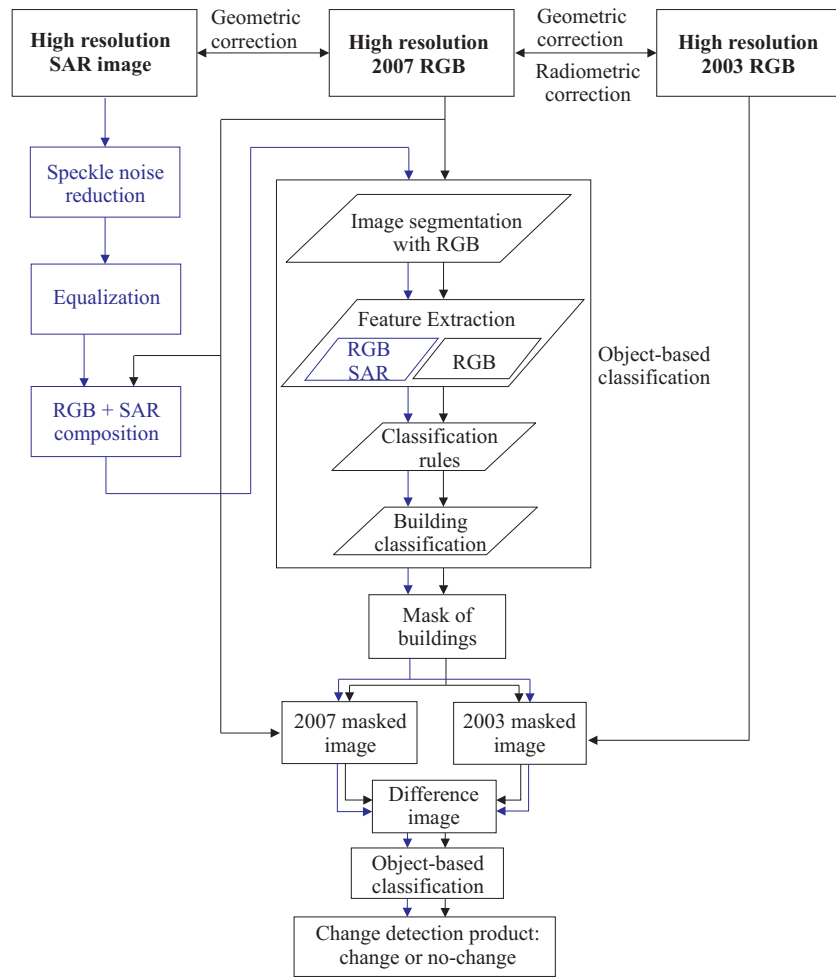


Figure 1: Flow diagram.

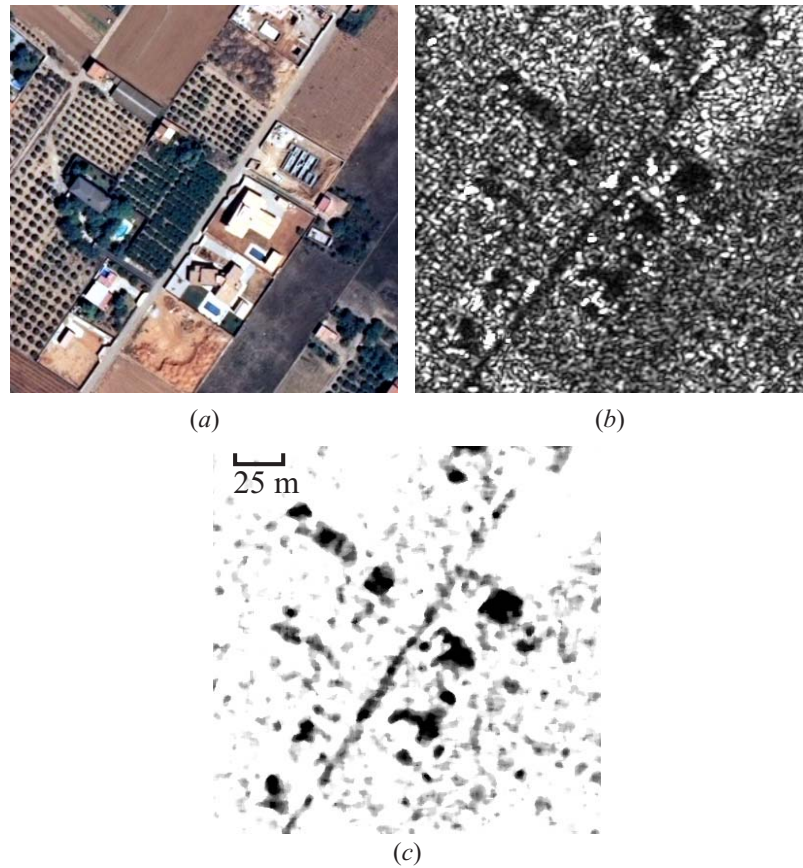


Figure 2: Portion of the study zone in the optical domain in (a), original high resolution SAR image in (b) and post-processed SAR image in (c).

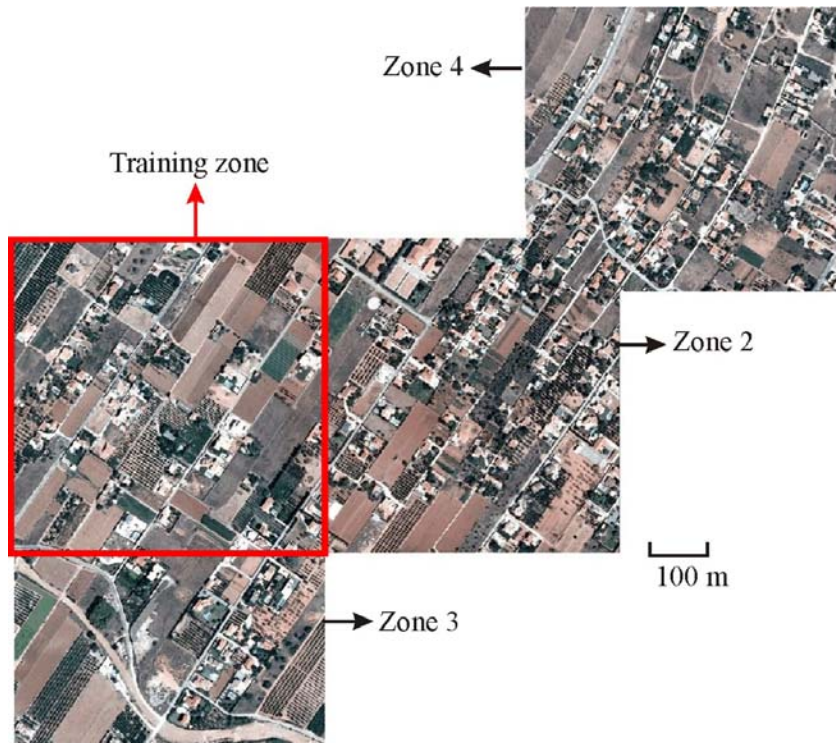


Figure 3: Zone of study in the RGB image acquired in 2007. The upper left corner of the training zone is located at  $40^{\circ}24'50''$  N  $0^{\circ}24'28''$  E.



Figure 4: A detail of the building classification contours shown over the 2007 scene using RGB bands in (a) and using RGB and SAR bands in (b).



Figure 5: A detail of the change detection results obtained by the RGB-SAR procedure. The changes are represented by a red star over the 2003 image (a) and over the 2007 image (b).



Figure 6: A detail of the change detection results shown on the 2003 in (a-c) and 2007 scene in (b-d), using only the RGB image in (a-b) and using the RGB-SAR data in (c-d). True changes are represented by a red star, whereas the results are marked by a blue circle.